SUPPLEMENTARY APPENDIX

PD-L1+ tumor-associated macrophages and PD-1+ tumor-infiltrating lymphocytes predict survival in primary testicular lymphoma

Marjukka Pollari,[1,2] Oscar Brück,[3] Teijo Pellinen,[4] Pauli Vähämurto,[1,5] Marja-Liisa Karjalainen-Lindsberg,[6] Susanna Mannisto,[1,5] Olli Kallioniemi,[4,7] Pirkko-Liisa Kellokumpu-Lehtinen,[2,8] Satu Mustjoki,[3,9] Suvi-Katri Leivonen[1,5] and Sirpa Leppä[1,5]

[1]Research Program Unit, Faculty of Medicine, University of Helsinki, Finland; [2]Department of Oncology, Tampere University Hospital, Finland; [3]Hematology Research Unit Helsinki, Department of Clinical Chemistry and Hematology, University of Helsinki, Finland; [4]Institute for Molecular Medicine Finland (FIMM), Helsinki, Finland; [5]Department of Oncology, Comprehensive Cancer Center, Helsinki University Hospital, Finland; [6]Department of Pathology, Helsinki University Hospital, Finland; [7]Science for Life Laboratory, Karolinska Institutet, Department of Oncology and Pathology, Solna, Sweden; [8]Faculty of Medicine and Life Sciences, University of Tampere, Finland; [9]Department of Hematology, Comprehensive Cancer Center, Helsinki University Hospital, Finland

 doi:10.3324/haematol.2018.197194

Received: May 6, 2018.

Accepted: July 16, 2018.

Pre-published: July 19, 2018.

Correspondence: sirpa.leppa@helsinki.fi

Supplementary material

PD-L1$^+$ tumor-associated macrophages and PD-1$^+$ tumor infiltrating lymphocytes predict survival in primary testicular lymphoma

Marjukka Pollari[1,2], Oscar Brück[3], Teijo Pellinen[4], Pauli Vähämurto[1,5], Marja-Liisa Karjalainen-Lindsberg[6], Susanna Mannisto[1,5], Olli Kallioniemi[4,7], Pirkko-Liisa Kellokumpu-Lehtinen[2,8], Satu Mustjoki[3,9], Suvi-Katri Leivonen[1,5] and Sirpa Leppä[1,5]

[1]Research Program Unit, Faculty of Medicine, University of Helsinki, Helsinki, Finland;
[2]Department of Oncology, Tampere University Hospital, Tampere, Finland;
[3]Hematology Research Unit Helsinki, Department of Clinical Chemistry and Hematology, University of Helsinki, Helsinki, Finland;
[4]Institute for Molecular Medicine Finland (FIMM), Helsinki, Finland;
[5]Department of Oncology, Comprehensive Cancer Center, Helsinki University Hospital, Helsinki, Finland;
[6]Department of Pathology, Helsinki University Hospital, Helsinki, Finland;
[7]Science for Life Laboratory, Karolinska Institutet, Department of Oncology and Pathology, Solna, Sweden;
[8]Faculty of Medicine and Life Sciences, University of Tampere, Tampere, Finland;
[9]Department of Hematology, Comprehensive Cancer Center, Helsinki University Hospital, Helsinki, Finland

Supplementary methods

Multiplex Immunohistochemistry (mIHC)

General. TMA blocks were cut in 3.5 µm sections on objective slides, which were dried overnight at +37°C and stored for short-term use at +4°C. All consecutive phases were performed in room temperature unless otherwise specified. Protein blocking and antibody incubations were performed in a humid chamber. Slides were washed three times with 0.1% Tween-20 (Thermo Fisher Scientific) diluted in 10 mM Tris-HCL buffered saline pH 7.4 (TBS) after peroxide block, antibody incubations, and fluorochrome reaction. The primary antibodies are listed in Supplementary Table 1.

Tissue preparation. Slides were deparaffinized in xylene and rehydrated in graded ethanol series and H_2O. Heat-induced epitope retrieval (HIER) was carried out in 10 mM Tris-HCl - 1 mM EDTA buffer (pH 9) in +99°C for 20 min (PT Module, Thermo Fisher Scientific, Waltham, MA). Peroxide activity was blocked in 0.9% H_2O_2 solution for 15 min, and protein block performed with 10% normal goat serum (TBS-NGS) for 15 min.

Fluorescence staining. Primary antibodies were diluted in protein blocking solution and incubated for 1 h 45 min. Thereafter, secondary anti-mouse or anti-rabbit horseradish peroxidase-conjugated (HRP) antibodies (Immunologic, Netherlands) diluted 1:1 with washing buffer were applied for 45 min. Tyramide signal amplification (TSA) Alexa Fluor 488 (PerkinElmer, Waltham, MA) diluted in TBS was applied on the slides for 10 min. Primary antibodies were denaturated and enzymatic activity of secondary antibody HRP was quenched by repeating HIER. Thereafter, peroxide and protein block were repeated, followed by application of a different primary antibody, matching HRP-conjugated secondary antibody diluted 1:3 with washing buffer and TSA Alexa Fluor 555 (PerkinElmer). Again, HIER, peroxide block and protein block were repeated. Then, the slides were incubated with two additional primary antibodies immunized in different species overnight in +4°C. Next, AlexaFluor647 and AlexaFluor750 fluorochrome-conjugated secondary antibodies (Thermo Fisher Scientific) diluted in 1:150 and DAPI (Roche) counterstain diluted 1:250 in washing buffer were applied for 45 min. Last, we applied ProLong Gold mountant (Thermo Fisher Scientific) and a coverslip on the slides.

Denaturation test. In order to minimize false positive signal from antibody cross-reactions during the mIHC procedure, we required that primary antibodies selected for mIHC must be completely denatured during the HIER step between staining rounds. Therefore, the denaturation properties of all primary antibodies were examined by performing an additional HIER step between primary and secondary antibody incubation. Antibodies not denaturing completely were detected with Cy5 and Cy7 fluorescence probes, which do not require denaturation.

Imaging. Fluorescent images were acquired with the AxioImager.Z2 (Zeiss, Germany) microscope equipped with Zeiss Plan-Apochromat 20x objective (NA 0.8), CoolCube1 CCD camera (MetaSystems, Germany), PhotoFluor LM-75 (89 North) metal-halide light source and Zeiss EPLAX VP232-2 power supply. DAPI, FITC, Cy3, Cy5, and Cy7 filters with compatible LED light sources were used and exposure times for all fluorescence channels were optimized visually for fluorescence imaging. Scanned images were acquired and were converted to JPEG2000 format (95% quality) for image analysis to reduce memory demand.

Image analysis. The quality of gray-scale images of each TMA spot was first assessed and few images were discarded due to blurred focusing or unsuccessful image registration caused mainly by air bubbles in mounting media or shattered tissue, respectively. In the image analysis, DAPI-

counterstained nuclei were segmented with adaptive Otsu thresholding, clumped objects separated by intensity patterns and cells segmented with nuclei contour expansion. We used the machine-learning platform CellProfiler 2.1.2 for cell segmentation, intensity measurements (upper quartile intensity) and immune cell classification. We computed marker colocalization with the single-cell analysis software FlowJo v10 (FlowJo LLC.). The optimal gate coordinates were ensured by visualising matching cells with CellProfiler.

Data analysis Spots with less than 5000 cells were excluded from the analysis. Different cell types were quantified as proportion to all cells (e.g. number of $CD68^{+}PD\text{-}L1^{+}$ TAMs to all cells in a TMA spot). Duplicate spots from the same patient were merged by the mean value of each cell type and their immunophenotype.

Supplementary Figures

Supplementary Figure 1.

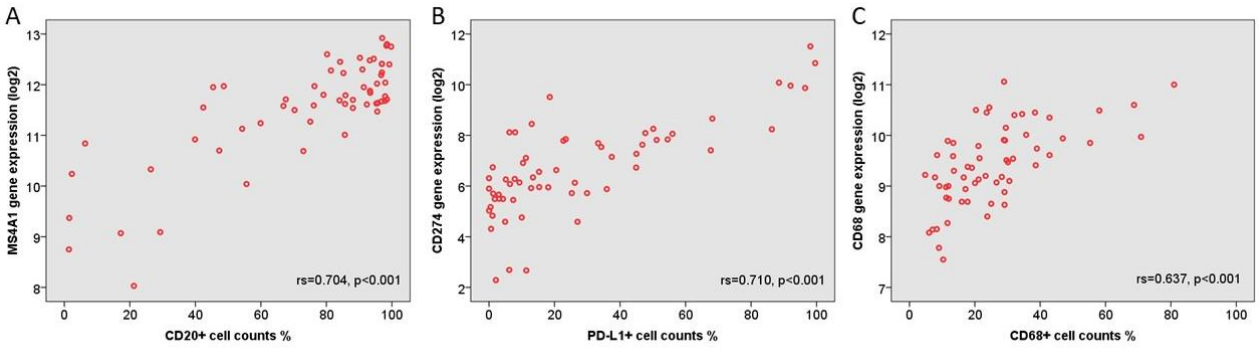

Correlation between gene expression and immunohistochemistry (IHC). A-C) Correlations between *MS4A1* (A), *CD274* (B), and *CD68* (C) mRNA levels with the corresponding cell counts in mIHC were determined by Spearman rank analysis.

Supplementary Figure 2.

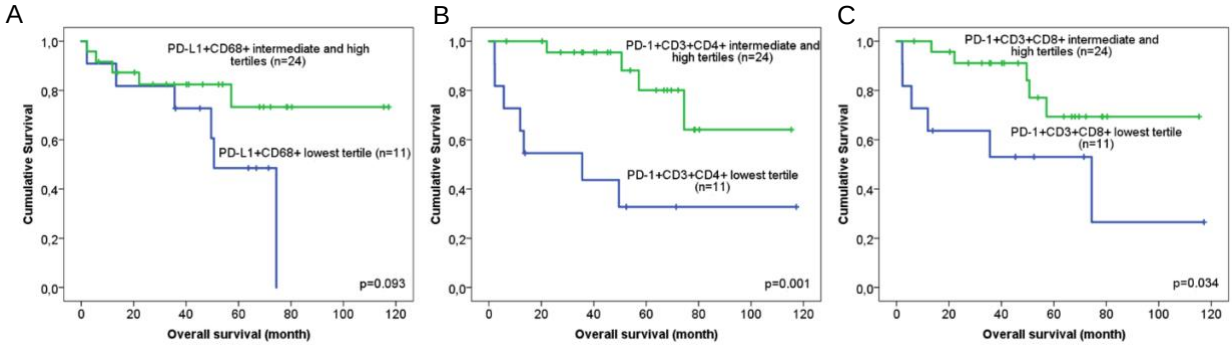

Association of the immune cell subtypes with survival among the rituximab treated patients. Cell immunophenotypes were determined by mIHC from 35 PTL patients treated with rituximab. Patients were stratified into three equal subgroups (high, intermediate and low), based on tertiles of PD-L1$^+$CD68$^+$ TAM, PD-1$^+$CD3$^+$CD4$^+$ T-cell, and PD-1$^+$CD3$^+$CD8$^+$ T-cell counts, and the intermediate and high groups were merged based on the data from the whole cohort of 74 patients. Kaplan-Meier plots depict survival differences between the PD-L1$^+$CD68$^+$ (A), PD-1$^+$CD3$^+$CD4$^+$ (B), and PD-1$^+$CD3$^+$CD8$^+$ (C) groups.

Supplementary tables

Supplementary Table 1. Antibody panels.

Theme	GFP	Cy3	Cy5	Cy7
T-cells	PD1[a]	CD3	CD8	CD4
Macrophages	c-MAF	PD-L1	PD-L2	CD68
B-cells and macrophages	PD-1	PD-L1	CD163	CD20

[a]Antibodies: PD-1 (clone PDCD1) LsBio, CD3 (clone EP449E) Abcam, CD8 (clone C8/144B) Abcam, CD4 (clone EPR6855) Abcam, cMAF (clone EPR16484) Abcam, PD-L1 (clone E1L3N) Cell Signaling, PD-L2 (polyclonal) Sigma, CD68 (clone KP1) Abcam, CD20 (clone L26) BioSB, CD163 (clone EPR14643), Abcam.

Supplementary Table 2. Correlations of the PD-1$^+$ TIL and PD-L1$^+$ TAM counts.

Cell immunophenotype	Spearman rho	p-val
$CD3^+CD4^+$ *vs.* $PD\text{-}L1^+CD68^+$	0.699	<0.001
$CD3^+CD8^+$ *vs.* $PD\text{-}L1^+CD68^+$	0.640	<0.001
$PD\text{-}1^+CD3^+CD4^+$ *vs.* $PD\text{-}L1^+CD68^+$	0.496	<0.001
$PD\text{-}1^+CD3^+CD8^+$ *vs*. $PD\text{-}L1^+CD68^+$	0.461	<0.001